special communication

Wavelet transform to quantify heart rate variability and to assess its instantaneous changes

VINCENT PICHOT,[1] JEAN-MICHEL GASPOZ,[2] SERGE MOLLIEX,[3] ANESTIS ANTONIADIS,[4] THIERRY BUSSO,[1] FRÉDÉRIC ROCHE,[1] FRÉDÉRIC COSTES,[1] LUC QUINTIN,[5] JEAN-RENÉ LACOUR,[6] AND JEAN-CLAUDE BARTHÉLÉMY[1]

[1]*Laboratoire de Physiologie-Groupement d'Intérêt Public Exercice, Université de Saint-Etienne, Saint-Etienne 42055;* [3]*Département d'Anesthésie et Réanimation, Hôpital Universitaire, Saint-Etienne 42055;* [4]*Département de Statistiques, Université Joseph Fourier, Grenoble 38041;* [5]*Laboratoire de Physiologie de l'Environnement, Unité de Recherche Associée, Centre National de la Recherche Scientifique, 1341, Hôpital Universitaire Rockefeller, Lyon 69373; and* [6]*Laboratoire de Physiologie-GIP Exercice, Université Lyon I, Lyon, France 69921; and* [2]*Département de Médecine Interne, Hopitaux Universitaires de Genève, Geneva, Switzerland 1211*

Pichot, Vincent, Jean-Michel Gaspoz, Serge Molliex, Anestis Antoniadis, Thierry Busso, Frédéric Roche, Frédéric Costes, Luc Quintin, Jean-René Lacour, and Jean-Claude Barthélémy. Wavelet transform to quantify heart rate variability and to assess its instantaneous changes. *J. Appl. Physiol.* 86(3): 1081–1091, 1999.—Heart rate variability is a recognized parameter for assessing autonomous nervous system activity. Fourier transform, the most commonly used method to analyze variability, does not offer an easy assessment of its dynamics because of limitations inherent in its stationary hypothesis. Conversely, wavelet transform allows analysis of nonstationary signals. We compared the respective yields of Fourier and wavelet transforms in analyzing heart rate variability during dynamic changes in autonomous nervous system balance induced by atropine and propranolol. Fourier and wavelet transforms were applied to sequences of heart rate intervals in six subjects receiving increasing doses of atropine and propranolol. At the lowest doses of atropine administered, heart rate variability increased, followed by a progressive decrease with higher doses. With the first dose of propranolol, there was a significant increase in heart rate variability, which progressively disappeared after the last dose. Wavelet transform gave significantly better quantitative analysis of heart rate variability than did Fourier transform during autonomous nervous system adaptations induced by both agents and provided novel temporally localized information.

Fourier transform; atropine; propranolol; autonomous nervous system

ADAPTATIONS OF THE ACTIVITY of the autonomous nervous system have been widely studied through heart rate variability, which was first described by Hales (10) in 1733, by extracting the physiological rhythms embedded in its signal (28). Indeed, physiological regulations, particularly blood pressure adaptations, pharmacological responses to many drugs, as well as numerous clinical applications, have been explored through its use. This interest is notably reinforced by the known direct relationship between autonomous nervous system tone and heart rate (20), sinoatrial stretch (12), or myocardial contractility (6). Different physiological parameters can be addressed, such as respiratory sinus arrhythmia (25) mediated by parasympathetic activity, thermoregulatory fluctuations in vasomotor tone (13, 19), and baroreflex control (3, 23). Hon and Lee (11) appreciated its clinical relevance for the first time in 1965; clinical applications today also describe the parallelism between the degree of heart rate variability and health status, including morbidity and mortality in cardiac diseases (4, 28).

Different mathematical methods have been used to analyze heart rate variability. Among these, Fourier transform is the one most commonly chosen (27, 28) but one that is, however, limited to stationary signals. With this mathematical transform, global representative indexes of heart rate variability have to be calculated as a set of cumulate spectrum powers contained in a given number of R wave-to-R wave (R-R) intervals, which prevents temporal localization of sudden changes in the behavior of the R-R signal. To overcome these limitations, we applied wavelet transform, which offers two complementary interesting features (2, 9, 16, 32). First, wavelet transform allows a temporally localized sliding analysis of the signal, thus giving access at any time to the status of heart rate variability, as, for example, when the balance of autonomous nervous system equilibrium is suddenly modified by acute clinical situations (15, 16, 29, 32) such as anesthesia or pharmacological interventions (8). Second, the shape of the wavelet transform-analyzing equation differs from the fixed sinusoidal shape of the Fourier transform and can be designed to better fit the shape of the analyzed signal, allowing a better quantitative measurement.

To compare the respective yields of these two mathematical methods in analyzing heart rate variability, we assessed their respective ability to quantify, as well as qualify, a shift in autonomous nervous system equi-

librium in response to the administration of increasing doses of atropine and propranolol.

METHODS

Subjects. Six sedentary male subjects, aged 27.7 ± 3.3 yr (mean weight 69.8 ± 8.1 kg, mean height 1.75 ± 0.10 m), received increasing intravenous doses of atropine and of propranolol while being monitored by using a Holter electrocardiogram recorder.

All subjects were free of any cardiac abnormalities and did not receive any treatment. The study was approved by the ethical committee of the University Hospital of Lyon, France. All subjects were volunteers and had signed an informed consent form.

Pharmacological protocol. All subjects were familiarized with the environment of the laboratory. They were requested to avoid alcohol and caffeine before and during the recording periods and to not perform heavy physical exercises during the preceding 24 h. An intravenous catheter was inserted into a large forearm vein 1 h before the beginning of the recordings. The subjects were then recorded in the supine position in a quiet room, which was exclusively reserved for the study. All recordings were started at 8 AM.

During the atropine injection period, an anesthesiologist continuously monitored the subjects and could follow through a monitor the effects of the drug on the electrocardiogram.

Each atropine injection was performed in ~5 s and flushed through with 20 ml of normal saline. Four (1 μg/kg), three (2 μg/kg), and five (5 μg/kg) doses of atropine were injected consecutively at 20-min intervals. The doses were chosen to obtain cumulate doses equal to 1, 2, 3, 4, 6, 8, 10, 15, 20, 25, 30, and 35 μg/kg, respectively, without correction for the dilution or elimination of the previous doses.

On a different day, a single bolus of 15 μg/kg of atropine was also administrated once in one subject.

On another day, three consecutive boluses (50, 50, and 100 μg/kg) of propranolol were injected consecutively at 20-min intervals to progressively obtain complete blockade, given the large volume of distribution and the fast clearance of the drug.

Recording procedure. The Holter recording procedures began 1 h before the first injection of atropine or propranolol and were prolonged for a 24-h period. Each intravenous administration was indicated on the Holter tape recorder by pressing the event button. Twenty minutes after the last injection, subjects were allowed to move about the laboratory.

R-R interval analysis. The electrocardiographic Holter system (StrataScan 563, Del Mar Avionics, Irvine, CA) allowed extraction of the list of R-R intervals with a precision of 1/128 s. The length of each R-R interval was manually validated during this step.

The mathematical analysis was made on a PowerMacintosh by using MatLab and the dedicated toolbox software Wavelab.

Fourier transform. This analysis is based on the fact that data present with a stationary organization and are a combination of sinusoidal functions (26, 27). Thus the algorithms of analysis are searching for sinusoidal similarities in the signal. Unlike wavelet analysis, which is described below (see *Wavelet transform*), the search does not indicate the localization of the particular frequency along the observed signal, but, instead, provides a cumulate spectrum power of a particular frequency, i.e., corresponding to the number of occurrences of the given sinusoidal function, without indicating when it occurred. In our study, this analysis was conducted over periods of 256 consecutive R-R intervals. The spectrum power was calculated on ultralow (ULF; 0.0–0.04 Hz), low (LF: 0.04–0.15 Hz), and high (HF; 0.15–0.40 Hz) frequencies, and the low-high index was derived to obtain the autonomic nervous system balance. For the quantification measurements, we separately calculated variability on consecutive 20-min steady-state periods, corresponding to the consecutive doses of atropine and propranolol.

Wavelet transform. This analysis is devoted to the extraction of characteristic frequencies, or specific oscillations, of a signal that, in our study, was composed of the consecutive intervals between R-Rs.

Unlike Fourier, wavelet transform is usually devoted to the analysis of nonstationary signals. Thus there is no prerequisite over the stability of the frequency content along the signal analyzed. Conversely to Fourier, wavelet analysis allows one to follow the temporal evolution of the spectrum of the frequencies contained in the signal.

Like Fourier or Laplace transforms, the continuous wavelet transform is an integral transform. The decomposition of a signal by wavelet transform requires a Ψ function adequately regular and localized, called the "Mother function." Starting from this initial function, a family of functions is built by dilatation and translocation, which constitute the so-called "wavelet frame." This frame is defined as follows

$$\Psi_{a,b} = 1/\sqrt{|a|} \cdot \Psi[(x - b)/a] \qquad a \in \mathbb{R}^* \qquad b \in \mathbb{R}$$

where a is a real number different from zero, b is a real number, and x is the abscissa on which the signal is analyzed.

The wavelet transform of a signal f is defined as

$$W_{f(a,b)} = <f,\Psi a,b> \qquad a \in \mathbb{R}^* \qquad b \in \mathbb{R}$$

where $<, >$ is the L^2 scalar product of f and $\Psi_{a,b}$, i.e., $\int f(x) \cdot \Psi_{a,b}(x) \cdot dx$.

The calculation of this scalar product is the analysis of f by the wavelet Ψ. It allows a local analysis of f and evidences the presence of all members of the family, which are all scaled representatives of the Mother function. Indeed, if the Mother wavelet is 0 out of $[-m,+m]$, then $\Psi_{a,b}$ is 0 out of $[-m|a|+b, m|a+b]$, where m is a real number greater than zero ($m \in \mathbb{R} \cdot +$). As a consequence, the value of $W_{f(a,b)}$ depends on the value of f near b, with a weight proportional to a, where W is wavelet transform. Quantitatively, the value of $W_{f(a,b)}$ is representative of the importance of the concordance of $\Psi_{a,b}$ to f near b at the a level. Thus wavelet analysis can be considered as a local Fourier analysis performed at different separated levels.

The analysis amounts to sliding a window of different weights (corresponding to different levels) containing the wavelet function all along the signal. The weight characterizes a family member with a particular dilatation factor. The calculation of $W_{f(a,b)}$ gives a serial list of coefficients called "wavelet coefficients," which represent the evolution of the correlation between the signal f and the chosen wavelet at different levels of analysis (or different ranges of frequencies) all along the signal f (24).

A theorical example of wavelet analysis is represented in Fig. 1. The signal to be analyzed (Fig. 1, *top*) can be described as demonstrating three different behaviors; the first part contains a mixture of high- and low-frequency sinusoidal signals, whereas the last two parts are made up of a low- and a high-frequency signal, respectively. The signal is analyzed by using a wavelet base built with a Mother function called "Daubechies 4," represented in Fig. 1, *bottom right*. The wavelet analysis of this nonstationary signal allows one to follow the evolution of the presence of each frequency contained in the initial signal through time (Fig. 1, *bottom left*). Each wavelet coefficient is determined at its level. The first

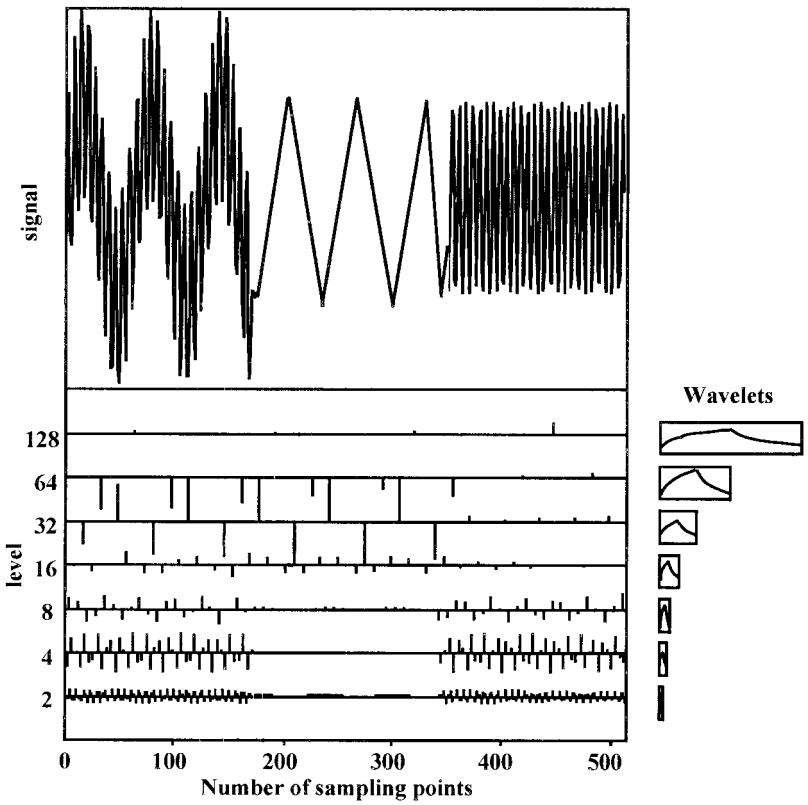

Fig. 1. Ability of wavelet analysis to show sudden variations along a time scale. *Right*: shape of analyzing wavelet for each level.

levels (2, 4, 8, ...) correspond to a wavelet analysis conducted with a small value of the dilatation factor, thus representing high-frequency variations in the signal. On the contrary, the last levels (..., 32, 64, 128) correspond to a wavelet analysis conducted with a large value of the dilatation factor, thus representing low-frequency variations in the signal. At any level, the larger the coefficients, the greater the correspondence between the original signal and the analyzing wavelet. This is illustrated by Fig. 2, which shows the consecutive 24-h R-R values plotted against time (Fig. 2, *top*) in a young normal subject and the corresponding levels and wavelet coefficients (Fig. 2, *bottom*).

In the application presented in this paper, the number of sampling points is the number of R-R intervals. To analyze the smallest modifications, the smallest scaled wavelet compares the length of two (2^1) consecutive R-R intervals; this gives the highest frequency analyzed. At the level immediately above, the analyzing wavelet is scaled to analyze the length variations of four (2^2) consecutive R-R intervals, the comparison being performed between the shape determined by the series of the four consecutive R-R intervals and the shape of the analyzing wavelet; the frequency analyzed at this level is halved compared with the previous level. Then, each time the analysis goes up a level, the set of R-R intervals analyzed is the next in the 2^{n+1} series of R-R intervals, and the frequency analyzed is halved. The maximum number of points that can be analyzed is limited to the last complete 2^n set of R-R intervals that can be extracted from the whole data set; the R-R intervals that cannot be included in such a 2^n set are not analyzed. Thus the number of levels is limited by this feature to $\log_2 n$, (n = number of sampling points), n being itself limited to values that are a power of 2. Given the ~100,000 R-R intervals recorded on a standard 24-h Holter, this allows a maximal number of 16 levels, or of 65,536 R-R

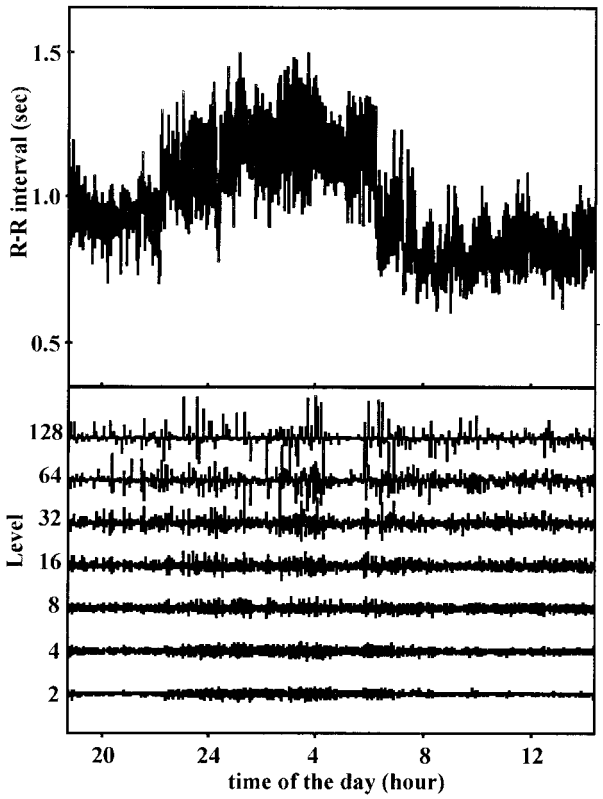

Fig. 2. Wavelet analysis (*bottom*) performed on a signal representing consecutive R wave-to-R wave (R-R) intervals in a normal subject during a 24-h period (*top*).

intervals, to be analyzed. From these, in the data presented, we retained only the seven levels bearing the highest frequencies; they were labeled *levels 2*, *4*, *8*, *16*, *32*, *64*, and *128*, respectively, the numbers corresponding to the width of the wavelet with which the R-R signal is compared. In other words, the shape drawn by the progressive lengthening or shortening of the successive R-R intervals is compared, at each analyzed level, with the shape of the analyzing wavelet.

In our analysis, we used the Daubechies 4 wavelet transform. For each record, the wavelet coefficients were calculated at each of the seven levels. Then we calculated the variability power, level by level, as the sum of squares of the coefficients at this level during a given time interval, i.e., in the case of the atropine and propranolol protocols, during consecutive 20-min periods, each corresponding to a given dose of atropine or propranolol, and, thus, to separate steady states. Therefore, we obtained, for each steady-state period, the variability power for each level. We chose a depth giving seven separate levels (2 ... 128). The frequencies representing each level can be calculated as 2/duration of the analyzed interval, depending on both the heart rate and the level analyzed.

The frequency value of a given level varies directly with the mean frequency of the R-R sample analyzed and can be calculated as [2/($n \times$ mean R-R interval)], n being the level, as labeled in our study. Wavelet power coefficients at *levels 2*, *4*, and *8* correspond approximately to the Fourier high frequencies (HF); wavelet power coefficients at *levels 16* and *32* correspond to the Fourier LF; and, finally, wavelet power coefficients at *levels 64* and *128* correspond to the Fourier ULF. A LF-to-HF ratio (LF/HF) was calculated as the ratio between the sum of the wavelet power coefficients at *levels 16* and *32* on one hand and the sum of the wavelet power coefficients at *levels 2*, *4*, and *8* on the other, to obtain a marker of autonomic nervous system equilibrium, as it is usually done with Fourier analysis.

Analysis of the atropine bolus procedure. This was intended to illustrate the response time of wavelet transform vs. Fourier transform after one bolus injection of atropine. First, a set of Fourier analyses was performed on the 256 consecutive R-R intervals before the bolus; then, this 256-R-R-interval window was progressively shifted to incorporate, at each step, 5 new R-R intervals, until all 256 R-R intervals belonged to the postinjection period. Second, a wavelet analysis was performed on the same sequence of R-R intervals.

Statistical analysis. Statistical analyses were performed with the sofware MATLAB, Statview, and SuperANOVA on a PowerMacintosh. A two-factor analysis of variance was performed with subjects and drug doses. $P < 0.05$ was considered significant.

RESULTS

Heart rate evolution. The first doses of atropine (1–3 μg/kg) determined a nonsignificant increase in R-R intervals, followed by a progressive decrease in R-R intervals with the next doses (4–35 μg/kg), compared with the reference period, which reached significance ($P < 0.05$) at the last dose only. After the last atropine dose, the R-R intervals progressively returned to a higher value (Table 1). Figure 3, *top*, shows the evolution of the R-R intervals of a subject during the protocol.

With the first dose of propranolol, there was a significant ($P < 0.05$) increase in the mean R-R intervals (Fig. 4, *top*, and Table 2), which progressively disappeared after the last dose.

Table 1. *Mean R-R values for 6 subjects during atropine administration and recovery time*

	R-R, s
Atropine, μg/kg	
0	0.809 ± 0.089
1	0.979 ± 0.378
2	1.044 ± 0.382
3	1.071 ± 0.404
4	0.946 ± 0.148
6	0.859 ± 0.148
8	0.792 ± 0.143
10	0.715 ± 0.102
15	0.656 ± 0.115
20	0.615 ± 0.079
25	0.601 ± 0.071
30	0.598 ± 0.080
35	0.585 ± 0.072*
Recovery, min	
+20	0.594 ± 0.056
+40	0.659 ± 0.071
+60	0.671 ± 0.070
+80	0.657 ± 0.066
+100	0.659 ± 0.088
+120	0.688 ± 0.077
+140	0.712 ± 0.087
+160	0.744 ± 0.096
+180	0.732 ± 0.108
+200	0.745 ± 0.111
+220	0.729 ± 0.073
+240	0.771 ± 0.103
Night	0.999 ± 0.204

Values are means ± SD. First value is the R-R value during the reference period; the next 12 values are R-R values during the successive 20-min periods for 1, 2, 3, 4, 6, 8, 10, 15, 20, 25, 30 and 35 μg/kg atropine, respectively; the next 12 values are successive R-R values during the recovery period, which were calculated for the next 12 consecutive 20-min intervals; the final value is the R-R value during the following night period. *$P < 0.05$.

Fourier analysis. Compared with the reference period, at any frequency analyzed, i.e., ULF, LF, and HF, neither the initial increase nor the later decrease in spectrum power measured during the consecutive steady states reached statistical significance during atropine administration. Only the LF/HF ratio showed some significant variations (Fig. 5, *bottom left*).

Propranolol administration determined a significant ($P < 0.05$) increase in spectrum power with the two last doses only, at the HF levels (Fig. 6, *left*). The LF/HF ratio was decreased, but not significantly.

Wavelet analysis. At the lowest doses of atropine (1–4 μg/kg or the first 4 steady states that followed), an initial significant increase in the power coefficients was observed for the five highest frequency levels, i.e., *levels 2*, *4*, *8*, *16*, and *32* (Fig. 5, *right*) compared with the reference period. After awhile, further increasing the dose of atropine significantly decreased the power coefficients of the following steady states. This decrease reached significance first for *levels 2* and *4* at a dose of 6 μg/kg, then for *level 8* at a dose of 10 μg/kg, and finally for *level 16* at a dose of 15 μg/kg (Fig. 5, *right*). At each

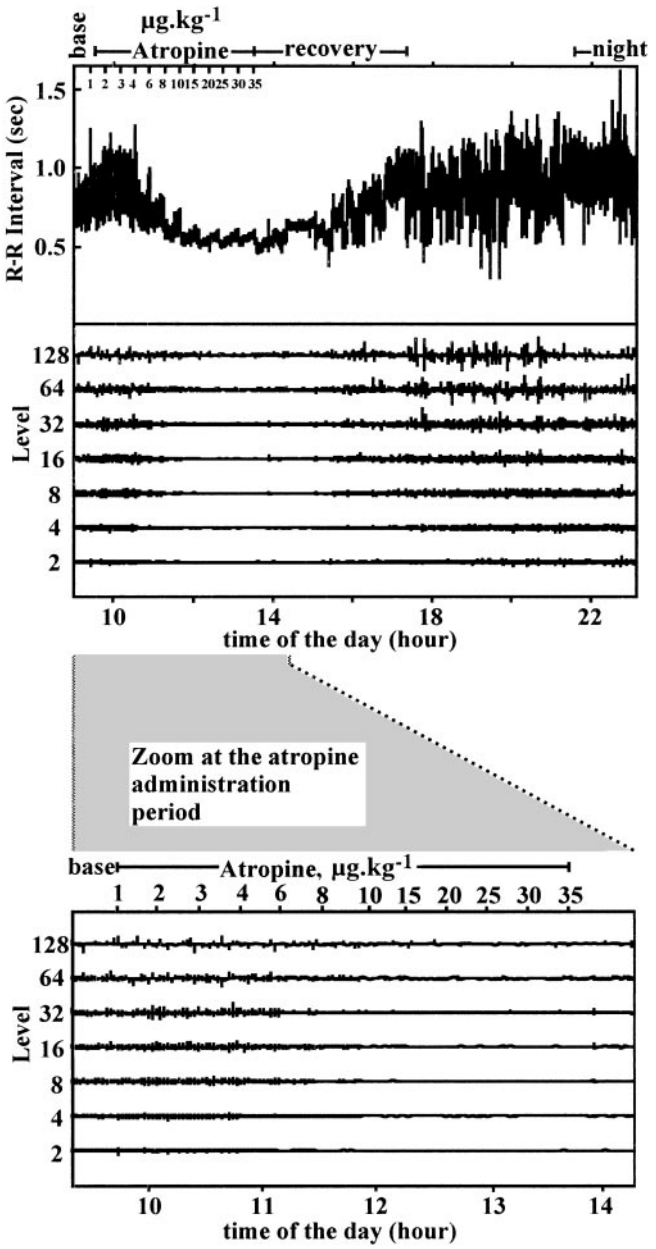

Fig. 3. Analysis of 1 signal representing consecutive R-R intervals by using Daubechies 4 wavelet in a normal subject receiving increasing doses of atropine. *Top*: R-R intervals during this period. Administration period is recognized, at the beginning, by a progressive lengthening of R-R intervals, followed by their progressive shortening. Administrations of atropine were made at 20-min intervals. Immediately following are results of wavelet transform analysis. Small vertical lines, power coefficients; length of these lines is proportional to correspondence between shapes of analyzed signal and analyzing equation. *Bottom*: individual example of atropine administration, with zoom at atropine administration period.

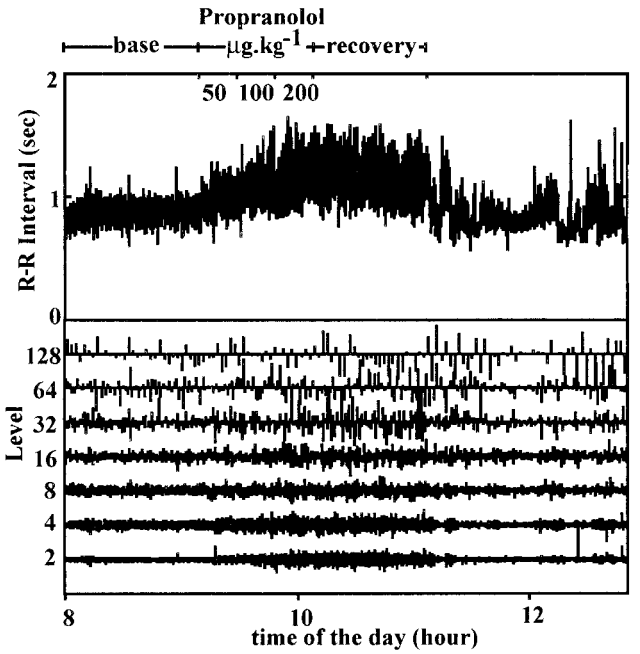

Fig. 4. R-R intervals and wavelet analysis (*top* and *bottom*, respectively) of propranolol administration protocol. *Top left* and *right*: normal R-R variability pattern. *Top middle*: propranolol administration period. Increases in mean R-R intervals and in variability are shown.

level, the decrease became deeper with the following doses. It is remarkable that, at any given level, the sooner a significant decrease was observed, the longer it took for the decrease to disappear. After the last injection, the order of reappearance of the coefficients was reversed compared with the order observed during their disappearance. Then, the power coefficients calculated during the night after the administration period were all significantly higher than during the preadministration period. During atropine administration, the wavelet LF/HF ratio demonstrated an increase that became significant for a dose of 15 µg/kg and remained significant 20 min after the last dose of 35 µg/kg (Fig. 7, *top*).

The analysis of the propranolol recordings showed a progressive and significant increase in the power coefficients for the highest frequency levels, particularly *levels 2* and *4*. For the two last doses (200 µg/kg of propranolol), the power coefficients at each level reached approximately the values obtained during the night period (Fig. 6, *right*). Compared with the initial value, power coefficients at *level 8* did not reach significant

Table 2. *Mean R-R values for 6 subjects during propranolol administration and recovery time*

	R-R, s
Propranolol, µg/kg	
0	0.868 ± 0.122
50	1.023 ± 0.126*
100	1.035 ± 0.142*
200	1.075 ± 0.141*
Recovery	0.842 ± 0.139
Night	1.026 ± 0.144*

Values are means ± SD. The 1st value is the R-R value during the reference period; the next 3 values illustrate the R-R values in the successive periods for 50, 100, and 200 µg/kg propranolol, respectively; the next value illustrates the R-R value during the recovery period; the final value illustrates the R-R during the following overnight period. *$P < 0.05$.

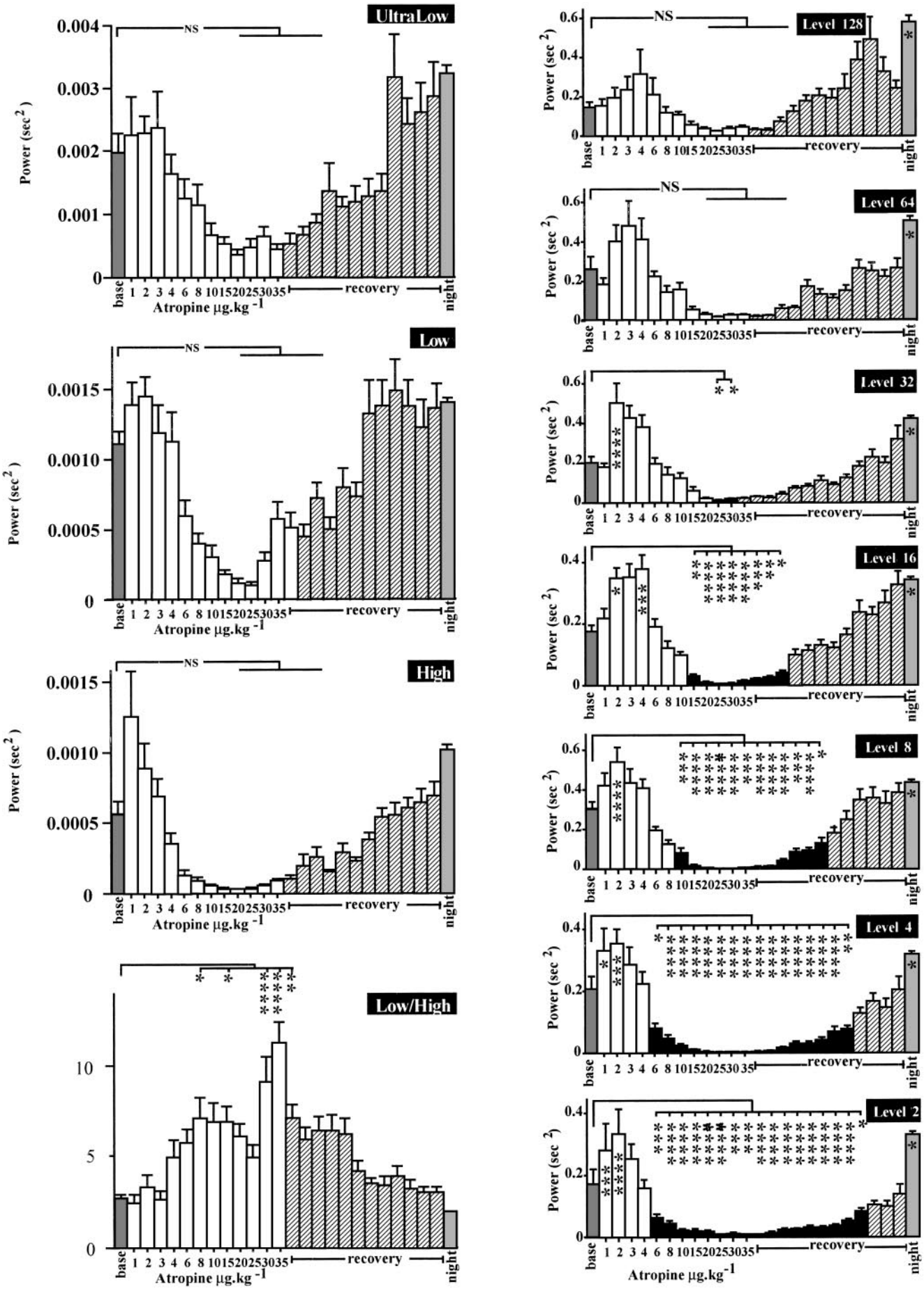

levels. The wavelet LF/HF ratio did not show significant differences (Fig. 7, *bottom*).

An individual example of atropine administration is illustrated in Fig. 3, *bottom*, with a zoom at the administration period, which better illustrates the progressive disappearance of the coefficients; in Fig. 3, *bottom*, the disappearance of the wavelet coefficients at a given level corresponds to the injection time (for example, their disappearance at *level 4* with a dose of 6 μg/kg of atropine). Wavelet analysis of an individual example of the propranolol recordings is also shown in Fig. 4, *bottom*.

Effect of the single bolus of atropine. The R-R intervals (Fig. 8*A*) demonstrated a shortening and a clear and abrupt decrease in variability ~15 s after the bolus injection.

Fourier transform analysis (Fig. 8*D*) demonstrated a decrease in the LF from 0.000400 to 0.000014 s^2 and in the HF from 0.000196 to 0.000004 s^2, all of which were very progressive. The Fourier LF/HF ratio demonstrated a progressive increase (Fig. 8*E*).

By contrast, wavelet transform clearly demonstrated a sudden fall in its coefficient values, at each frequency level, instantaneously accompanying the R-R interval changes (Fig. 8*B*). Similarly, the wavelet LF/HF ratio demonstrated an abrupt increase (Fig. 8*C*); this was followed by high-amplitude oscillations of this ratio. The initial elevation just before the administration could represent a true surge of sympathetic activity.

DISCUSSION

As hypothesized, wavelet transform performed differently from Fourier transform in analyzing heart rate variability. Two main features can be drawn from their comparison. First, from a qualitative point of view, wavelet analysis, because of its mathematical properties, continuously displayed and calculated the level of heart rate variability. Second, wavelet transform appeared to perform better than Fourier transform from a quantitative point of view in separating different levels of heart rate variability induced by a pharmacological intervention.

Up to now, adaptations of the cardiac autonomous nervous system have most often been evaluated by using Fourier transform of heart rate variability. The need to calculate the representative mean coefficients on a sufficient number of R-R intervals with that transform does not allow a precise detection of a sudden change in autonomous tone, and, thus, does not allow precise localization of one particular event in time (Fig. 8). Actually, because of this averaging process, the power coefficients resulting from that analysis, at a given frequency, are a mixture of events occurring at different times; even if a change occurs during the period analyzed, the mean power coefficients obtained only reflect the average of two different autonomous nervous system equilibriums. In contrast, wavelet analysis is able to calculate, at the highest frequency level, a representative coefficient of heart rate variability for each new set of two consecutive R-R intervals; this gives access to a precise, temporally localized status of heart rate variability for the parasympathetic as well as for the sympathetic drives, which is thus able to immediately reflect a shift in autonomous nervous system equilibrium. By using wavelet analysis, the update of heart rate variability coefficients at the highest frequency level only needs to integrate two new consecutive R-R intervals; the update of the frequency level immediately above must wait until four new R-R intervals have been integrated, and so forth. Thus the strength of wavelet analysis lies in the short delay needed to reflect a change in heart rate variability. This capacity to monitor instantaneous changes in autonomous nervous system tone will undoubtedly lead to new applications in physiology and therapeutics.

Fourier transform compares the shape of the signal to the shape of a sinusoidal function; thus any analyzed shape is always interpreted as a combination of several sinusoidal functions bearing different frequencies. Comparatively, wavelet transform allows the choice of an appropriate shape of the analyzing function to fit any particular signal. In our case, the Daubechies 4 wavelet better fit the point-to-point regulation of the R-R intervals by the autonomous nervous system. This probably explains the better quantitative separation in the power coefficients obtained by wavelet transform, as statistically observed during atropine administration. Undoubtedly, although the same statistical method was used for comparing the quantification represented by the power coefficients obtained from Fourier and wavelet transform of heart rate variability, the statistical differences obtained with the latter analysis were much more important. In any case, wavelet transform, at the highest doses of atropine, showed that the variability coefficients were entirely flattened out at any level. The question remains whether the analyzing shape of the wavelet equation should be adapted when different frequency levels are analyzed: it could be that, when the variability between series of different numbers of R-R intervals is analyzed, the ideal analyzing shape for the given length of a series, for example, 2 R-Rs, could be different from a shape fitting another length of a frequency or series, for example, 64 R-Rs.

Fig. 5. Fourier and wavelet transform analysis of heart rate variability during atropine administration. *Left*: Fourier indexes plotted against time during increase in atropine concentration and recovery period. *Right*: sum of squares of coefficients of wavelet transform analysis plotted against time during increase in atropine concentration and recovery period. Filled bars, reference value (base) averaged in a 20-min period; open bars, 20-min time interval in administration period; hatched bars, 20-min time intervals in recovery period; shaded bars, summary of 5 consecutive hours during following night period. NS, nonsignificant; Low/High, low frequency-to-high frequency ratio. * $P < 0.05$. ** $P < 0.01$. *** $P < 0.001$. **** $P < 0.0001$.

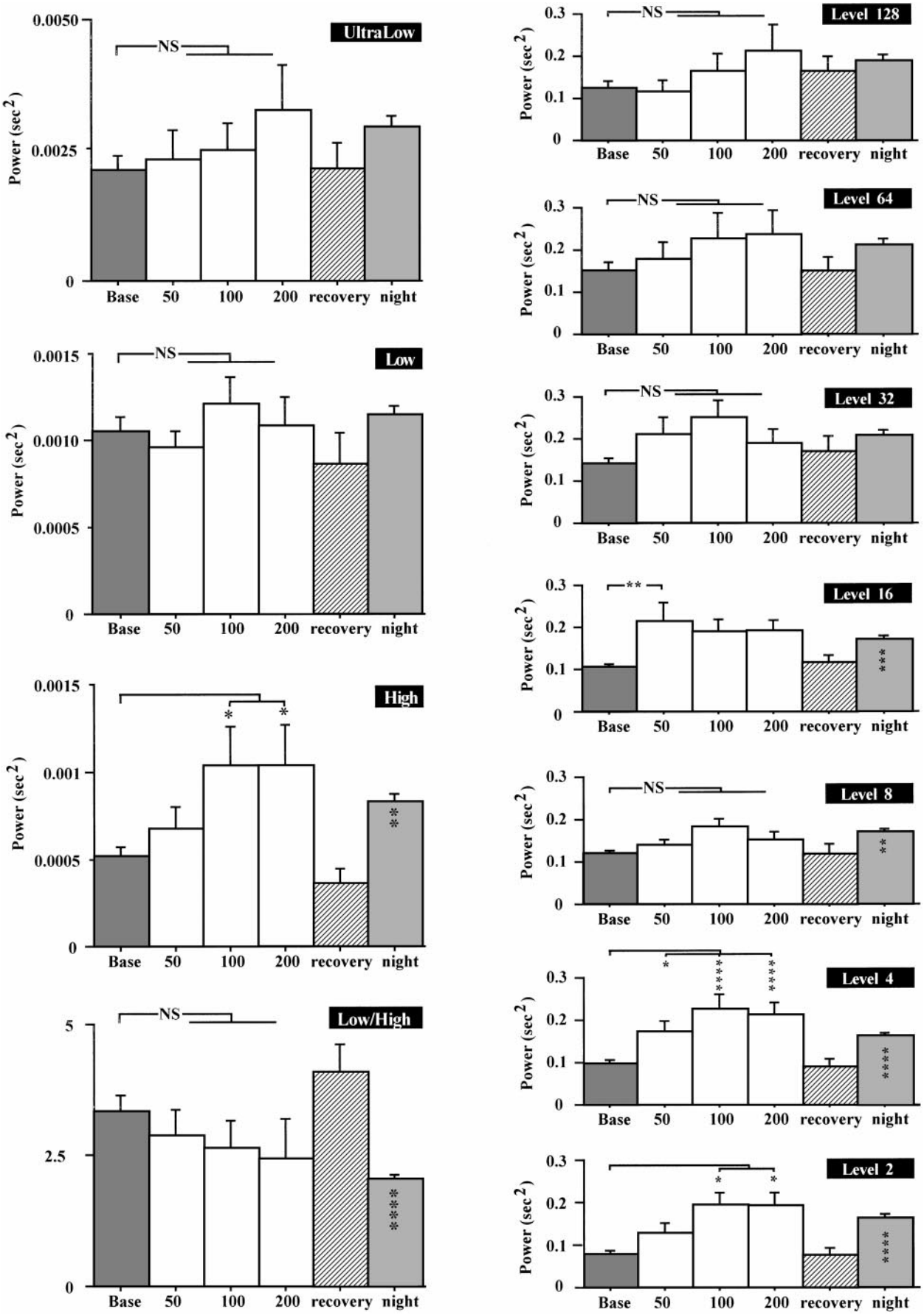

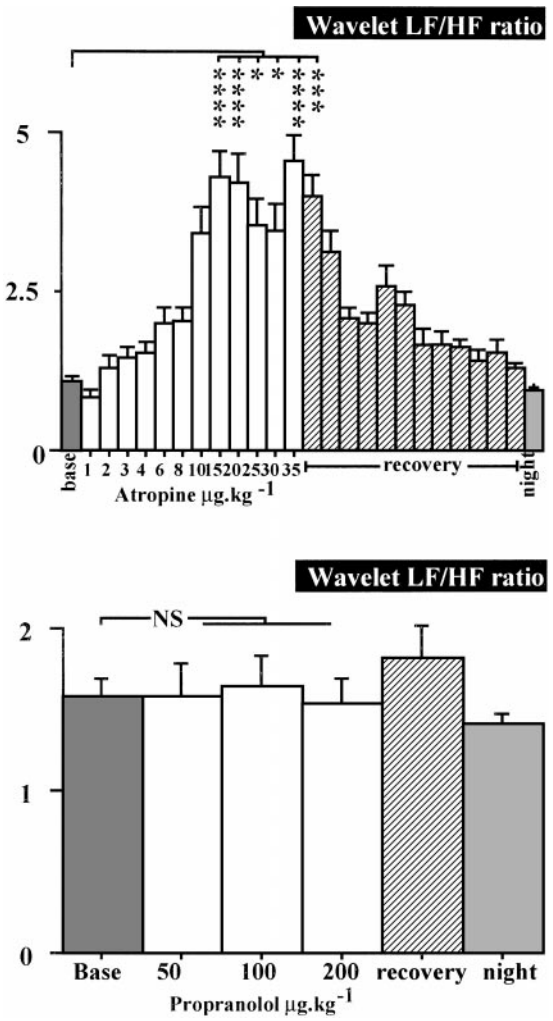

Fig. 7. Wavelet low frequency-to-high frequency ratio (LF/HF) during atropine and propranolol administration. *Top*: wavelet LF/HF ratio plotted against time during increase in atropine concentration, recovery period, and following night period. *Bottom*: wavelet LF/HF ratio plotted against time during consecutive doses of propranolol followed by recovery period and night period. $*P < 0.05$. $**P < 0.01$. $***P < 0.001$. $****P < 0.0001$.

Thus the physiological meaning of the wavelet coefficients represents, for the highest frequency, i.e., the variation observed between two consecutive R-R intervals, the ability of the autonomous nervous system to regulate the length of the second interval as an adaptation to the length of the first. As already described, heart rate variability is also assessed for higher combinations of intervals, these combinations being series of 2_n intervals. The local analysis allowed by wavelet analysis is, thus, performed for each of these combinations, allowing revelation of a modification in heart rate variability at each frequency and at any time. Furthermore, as shown in Figs. 1, 2, and 8, a clear graphical representation of these progressive temporal changes can be obtained. *Levels 2*, *4*, and *8* represent the frequencies that are attributed to parasympathetic activity, corresponding to the HF of Fourier indexes. The frequency band of the LF, which is an index of both parasympathetic and sympathetic activity, is represented by *levels 16* and *32*. On the whole, wavelet analysis is able to keep up a precise measurement of autonomous nervous system activity during transitory states (Figs. 6 and 8). Transients of sympathetic activity should also be precisely monitored by using wavelet transform but could be less evidenced than those of parasympathetic activity; this could be related to the fact that the LF power spectrum, and thus the LF/HF ratio, is not a pure index of sympathetic activity (7). Indeed, the LF/HF ratio did not show significant differences during propranolol administration (Fig. 7, *bottom*).

We followed step by step, in a single experiment, the whole array of the effects of atropine on heart rate variability up to the complete disappearance of these effects, as well as during the whole recovery period. As already shown, we observed that the smallest doses of atropine significantly increased heart rate variability (30). The effect of small doses of atropine on heart rate variability has been attributed to a central effect (17, 18), or a peripheral preference of the muscarinic presynaptic cholinergic receptors, which facilitate acetylcholine release (21). It has been demonstrated that, at higher doses, atropine attenuated or even abolished most of the frequency spectrum components of heart rate variability, as analyzed by Fourier transform (5, 14, 22, 31). Surprisingly, by using Fourier transform, even at the highest doses of atropine, we did not get a statistical difference from the reference level. As a matter of fact, we chose to assess the variations between the different periods by using ANOVA because we had more than two consecutive values to compare and also because we had to follow the variations over time; however, in the literature, the statistical comparison is generally done by using a paired *t*-test because only two different situations have to be compared, a baseline and an intervention period. Of course, when using paired *t*-tests on our Fourier transform results to compare the reference value to the intervention values, we got the same statistical differences as those already published; however, even in this case, wavelet transform allowed identification of more significant differences when ANOVA was used than Fourier transform when a paired *t*-test was used.

Fig. 6. Fourier and wavelet transform analyses of heart rate variability during propranolol administration. *Left*: Fourier indexes plotted against time during consecutive doses of propranolol followed by recovery and night periods. *Right*: sum of squares of coefficients of wavelet transform analysis plotted against time during consecutive doses of propranolol followed by recovery and night periods. Filled bars, reference value averaged in a 20-min period; open bars, 20-min time intervals in administration periods; hatched bars, 20-min time intervals in recovery period; shaded bars, summary of 5 consecutive hours in following night period. $*P < 0.05$. $**P < 0.01$. $***P < 0.001$. $****P < 0.0001$.

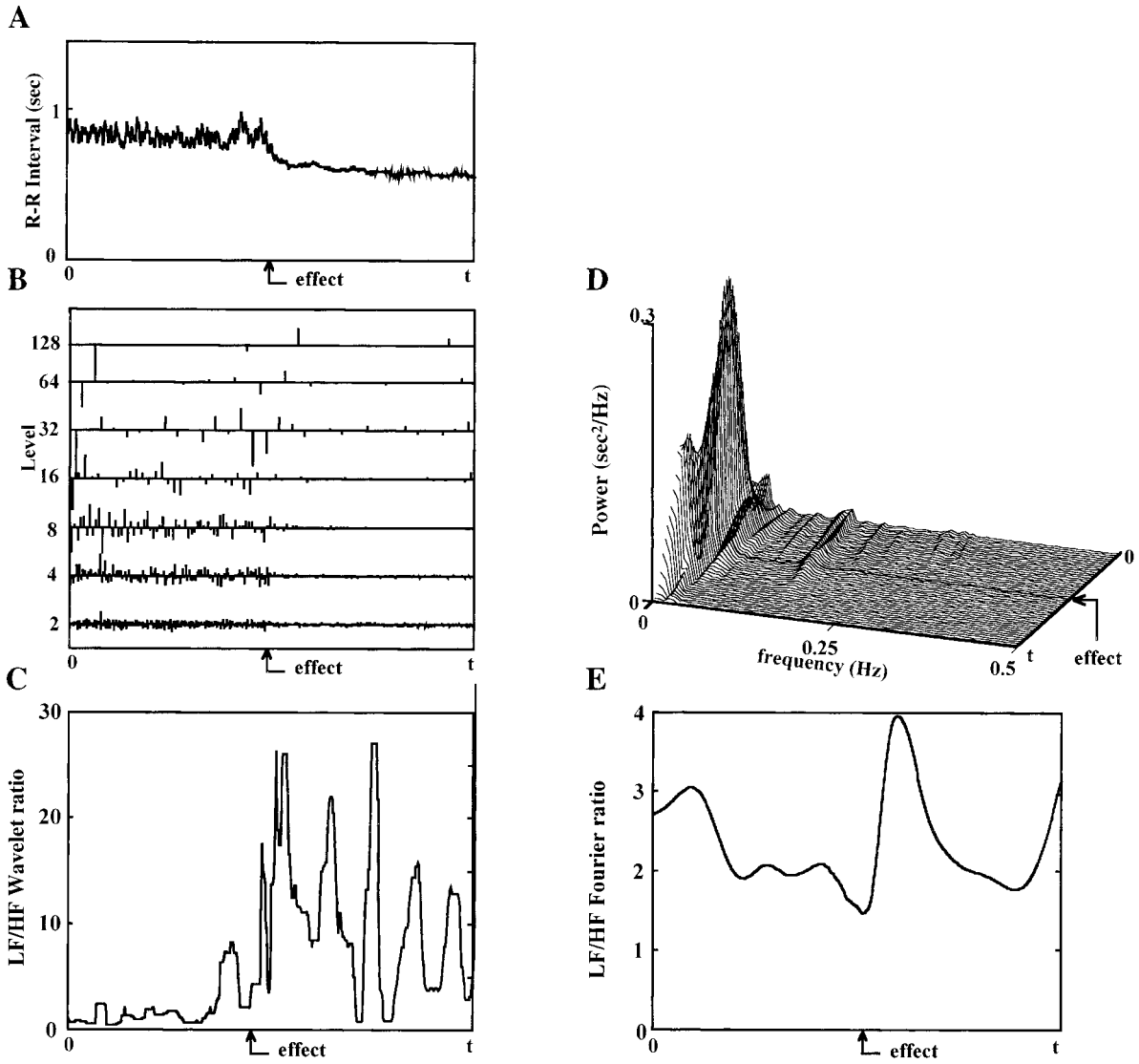

Fig. 8. Recording and analysis of effect of 1 single bolus of atropine; t, time. *A*: R-R intervals plotted against time. *Left*: normal R-R variability pattern; *right*: R-R shortening and near-abolition of R-R variability 15 s after injection. *B*: corresponding wavelet analysis. Analysis shows a tight correspondence between pattern of R-R interval values and wavelet coefficient values. *C*: wavelet LF/HF ratio plotted against time. *D*: evolution of Fourier spectrum calculated on 256 consecutive R-R intervals. Each new spectrum is calculated after a rightward shift, at each step, of 5 R-R intervals. *E*: corresponding Fourier ratio calculated on 256 R-R intervals. Effect (arrow) refers to same time point in *A*-*E*: abrupt fall in R-R length recorded 15 s after intravenous bolus.

In conclusion, the ability to present a local analysis of heart rate variability and to obtain a better quantification of it represents the major advantages of wavelet transform compared with Fourier transform. Fast autonomous nervous system adaptations could be precisely monitored by using the feature of temporally localized analysis. The relationship between parasympathetic tone and cardiac function (6) could probably also be further explored, benefiting both from the quantitative and temporal feature of this mathematical analysis. This additional novel and more precise temporal localization, brought by the ability of wavelet transform to analyze nonstationary signals, makes wavelet transform a promising tool for analyzing other temporary situations, such as progressive adaptations to exercise or progressive effects of pharmacological tests other than atropine, in which it could provide information not easily shown by more traditional methods (1).

We are indebted to Roland Thomas, Head of the Department of Medical Informatics, Saint-Etienne University Hospital, for valuable help. Del Mar Avionics, Inc., Irvine, CA, made accessible the R-R intervals lists from their Holter system.

This work was supported in part by a grant from the Région Rhône-Alpes (Eurodoc #L086840000).

Address for reprint requests: J.-C. Barthélémy, Laboratoire de Physiologie, CHU Nord-Niveau 6, F-42055 Saint-Etienne cedex 2, France (E-mail: JC.Barthelemy@univ-st-etienne.fr).

Received 13 November 1997; accepted in final form 17 October 1998.

REFERENCES

1. **Akay, M.** Introduction: wavelet transforms in biomedical engineering. *Ann. Biomed. Eng.* 23: 529–530, 1995.
2. **Akay, M., L. Landesberg, W. Welkowitz, Y. M. Akay, and D. Sapoznikov.** Carotid-cardiac interaction: heart rate variability during the unblocking of the carotid artery. In: *Interactive Phenomena in the Cardiac System*, edited by S. Sideman and R. Beyar. New York: Plenum, 1993, p. 365–372.
3. **Akselrod, S., D. Gordon, J. B. Madwed, N. C. Snidman, D. C. Shannon, and R. J. Cohen.** Hemodynamic regulation: investigation by spectral analysis. *Am. J. Physiol.* 249 (*Heart Circ. Physiol.* 18): H867–H875, 1985.
4. **Bigger, J. T., Jr., J. L. Fleiss, R. C. Steinman, L. M. Rolnitzky, W. J. Schneider, and P. K. Stein.** RR variability in healthy middle-aged persons compared with patients with chronic coronary artery disease or recent acute myocardial infarction. *Circulation* 91: 1936–1943, 1995.
5. **Cerutti, C., M.-P. Gustin, M. L. Paultre, C. Julien, M. Vincent, and J. Sassard.** Autonomic nervous system and cardiovascular variability in rats: a spectral analysis approach. *Am. J. Physiol.* 261 (*Heart Circ. Physiol.* 30): H1292–H1299, 1991.
6. **Douglass, P. S., L. L. O'Toole, and J. Woolard.** Regional wall motion abnormalities after prolonged exercise in the normal left ventricle. *Circulation* 82: 2108–2114, 1990.
7. **Eckberg, D. L.** Sympathovagal balance: a critical appraisal. *Circulation* 96: 3224–3232, 1997.
8. **Fei, L.** Effect of pharmacological intervention on heart rate variability: animal experiments and clinical observations. In: *Heart Rate Variability*, edited by M. Malik and A. J. Camm. Armonk, NY: Futura, 1995, p. 275–291.
9. **Graps, A.** An introduction to wavelets. *IEEE Comput. Sci. Eng.* 2: 50–61, 1995.
10. **Hales, S.** Statical essays. In: *Haemastaticks*, edited by Innings and Manby. London: 1733.
11. **Hon, E. H., and S. T. Lee.** Electronic evaluations of the fetal heart rate patterns preceding fetal death: further observations. *Am. J. Obstet. Gynecol.* 87: 814–826, 1965.
12. **Horner, S. M., C. F. Murphy, B. Coen, D. J. Dick, F. G. Harrison, and M. J. Vespalcova.** Contribution to heart rate variability by mechanoelectric feedback. Stretch of the sinoatrial node reduces heart rate variability. *Circulation* 94: 1762–1767, 1996.
13. **Hyndman, B. W., R. I. Kitney, and M. Sayers.** Spontaneous rhythms in physiologic control systems. *Nature* 233: 339–341, 1971.
14. **Japundzic, N., M. L. Grichois, P. Zitoun, D. Laude, and J. L. Elghozi.** Spectral analysis of blood pressure and heart rate in conscious rats: effects of autonomic blockers. *J. Auton. Nerv. Syst.* 30: 91–100, 1990.
15. **Jasson, S., C. Médigue, P. Maison-Blanche, N. Montano, L. Meyer, C. Vermeiren, P. Mansier, P. Coumel, A. Malliani, and B. Swynghedauw.** Instant power spectrum analysis of heart rate variability during orthostatic tilt using a time-/frequency-domain method. *Circulation* 96: 3521–3526, 1997.
16. **Jiménez, R., B. Günther, and A. Salazar.** Continuous wavelet transform of aortic pressure oscillations in anesthetized dogs: effects of 45° tilting. *Biol. Res.* 30: 53–64, 1997.
17. **Julu, P. O. O.** Central action of atropine on cardiovascular reflexes in humans. *J. Cardiovasc. Pharmacol.* 20: 332–336, 1992.
18. **Katona, P. G., D. Lipson, and P. J. Dauchot.** Opposing central and peripheral effects of atropine on parasympathetic cardiac control. *Am. J. Physiol.* 232 (*Heart Circ. Physiol.* 1): H146–H151, 1977.
19. **Kitney, R. I.** Entrainment of the human RR interval by thermal stimuli. *J. Physiol. (Lond.)* 252: 37P–38P, 1975.
20. **Levy, M. N., and P. J. Martin.** Neural control of the heart. In: *Handbook of Physiology. The Cardiovascular System. The Heart.* Bethesda, MD: Am. Physiol. Soc., 1979, sect. 2, vol. I, chapt. 16, p. 581–620.
21. **Löffelholz, K., and A. J. Pappano.** The parasympathetic neuroeffector junction of the heart. *Pharmacol. Rev.* 37: 1–24, 1985.
22. **Murphy, C. A., R. P. Sloan, and M. M. Myers.** Pharmacologic responses and spectral analyses of spontaneous fluctuations in heart rate and blood pressure in SHR rats. *J. Auton. Nerv. Syst.* 36: 237–250, 1991.
23. **Pagani, M., F. Lombardi, S. Guzzetti, O. Rimoldi, R. Furlan, P. Pizzinelli, J. Sandrone, G. Malfatto, S. Dell'Orto, E. Piccaluga, M. Turin, G. Baselli, S. Cerutti, and A. Maliani.** Power spectral analysis of heart rate and arterial pressure variabilities as a marker of sympatho-vagal interaction in man and conscious dog. *Circ. Res.* 59: 178–193, 1986.
24. **Percival, D. P.** On estimation of the wavelet variance. *Biomedika* 82: 619–631, 1995.
25. **Pomeranz, B., R. J. B. Macaulay, M. A. Caudill, I. Kutz, D. Adam, D. Gordon, K. M. Kilborn, A. C. Barger, D. C. Shannon, R. J. Cohen, and H. Benson.** Assessment of autonomic function in humans by heart rate spectral analysis. *Am. J. Physiol.* 248 (*Heart Circ. Physiol.* 17): H151–H153, 1985.
26. **Rompelman, O., A. J. R. Coenen, and R. I. Kitney.** Measurement of heart rate variability: Part 1-Comparative study of heart rate variability analysis method. *Med. Biol. Eng. Comput.* 15: 233–239, 1977.
27. **Sayers, B. M.** Analysis of heart rate variability. *Ergonomics* 16: 17–32, 1973.
28. **Task Force of the European Society of Cardiology and the North American Society of Pacing and Electrophysiology.** Heart rate variability. Standards of measurement, physiological interpretation, and clinical use. *Circulation* 93: 1043–1065, 1996.
29. **Tetzlaff, J. E., J. F. O'Hara, and H. J. Yoon.** Power spectral heart rate analysis to assess sympathetic tone during onset of spinal anaesthesia (Abstract). *Anaesthesia* 83: 3A: A476, 1995.
30. **Weise, F., K. Baltrusch, and F. Heydenreich.** Effect of low-dose atropine on heart rate fluctuations during orthostatic load: a spectral analysis. *J. Auton. Nerv. Syst.* 26: 223–230, 1989.
31. **Weise, F., F. Heydenreich, and U. Runge.** Contributions of sympathetic and vagal mechanisms to the genesis of heart rate fluctuations during orthostatic load: a spectral analysis. *J. Auton. Nerv. Syst.* 21: 127–134, 1987.
32. **Wiklund, U., M. Akay, and U. Niklasson.** Short-term analysis of heart rate variability by adapted wavelet transform. *IEEE Eng. Med. Biol. Mag.* 16: 113–118, 1997.